Articles published week of 30 AUGUST 2010
Volume 97 Number 9

APPLIED PHYSICS LETTERS

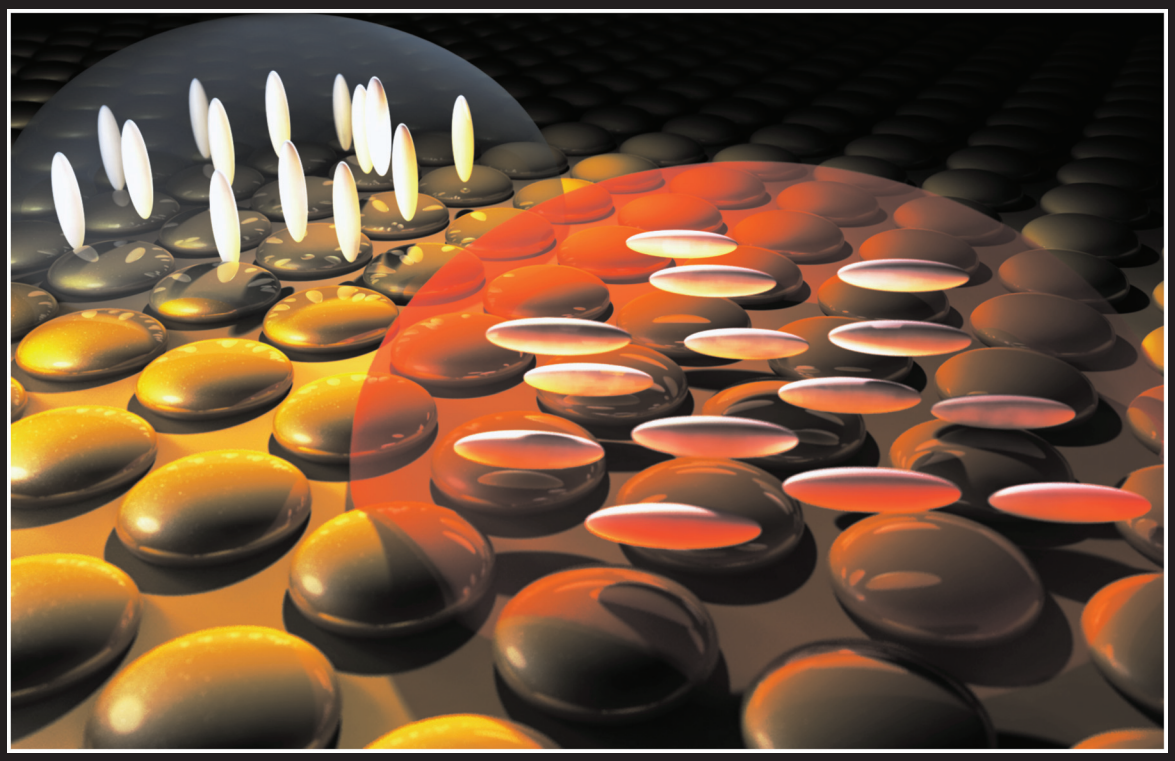

0003-6951(20100830)97:9;1-#

AIP

A frequency-addressed plasmonic switch based on dual-frequency liquid crystals

Yan Jun Liu,[1] Qingzhen Hao,[1,2] Joseph S. T. Smalley,[1] Justin Liou,[3] Iam Choon Khoo,[3] and Tony Jun Huang[1,a)]
[1]*Department of Engineering Science and Mechanics, The Pennsylvania State University, University Park, Pennsylvania 16802, USA*
[2]*Department of Physics, The Pennsylvania State University, University Park, Pennsylvania 16802, USA*
[3]*Department of Electrical Engineering, The Pennsylvania State University, University Park, Pennsylvania 16802, USA*

(Received 19 May 2010; accepted 11 June 2010; published online 30 August 2010)

A frequency-addressed plasmonic switch was demonstrated by embedding a uniform gold nanodisk array into dual-frequency liquid crystals (DFLCs). The optical properties of the hybrid system were characterized by extinction spectra of localized surface plasmon resonances (LSPRs). The LSPR peak was tuned using a frequency-dependent electric field. A ~4 nm blueshift was observed for frequencies below 15 kHz, and a 23 nm redshift was observed for frequencies above 15 kHz. The switching time for the system was ~40 ms. This DFLC-based active plasmonic system demonstrates an excellent, reversible, frequency-dependent switching behavior and could be used in future integrated nanophotonic circuits. © *2010 American Institute of Physics*.
[doi:10.1063/1.3483156]

Plasmonic resonances in metallic nanostructures have been attracting great interest due to their wide applications, including lasers,[1,2] waveguides,[3,4] microscopies,[5] and light-emitting diodes.[6,7] The photon-electron excitations allow one to confine the electromagnetic waves to nanoscale dimensions resulting in strong field confinement and enhancement.[8] To control the plasmonic resonances, various approaches have been used to change the features, sizes, and spacing of the metallic structures.[9–14] In comparison to these physical approaches, varying the surrounding's dielectric properties is a much more effective method.[15–21] The use of active materials as surroundings could provide a dynamic, continuous, and reversible change in the plasmonic resonances, coined as "active plasmonics."[22–24]

In this letter, we demonstrate a frequency-addressed active plasmonic system based on a uniform Au nanodisk array covered by nematic dual-frequency liquid crystal (DFLCs). Such DFLCs can change the sign of dielectric anisotropy either from positive to negative, or from negative to positive, when the frequency of the applied field changes,[25–28] thereby changing the plasmonic resonances. Both blueshift and redshift in the plasmonic resonances can be conveniently achieved.

In our experiments, a highly ordered gold nanodisk array on an indium-tin-oxide (ITO) glass substrate was fabricated according to the standard e-beam lithography procedures. In brief, a 120-nm-thick e-beam resist was spin-coated on the pretreated ITO glass substrate, followed by 3 min baking at 180 °C. Following that, a Au conductive film (~10 nm) was thermally deposited on the substrate in vacuum before exposure in the e-beam lithography system. After exposure, the Au film was removed using the Au Etchant TFA (Transene) for 30 s and the patterns were then developed in n-amyl acetate at 20 °C for 3 min, followed by immersing into methyl isobutyl ketone:isopropanol (IPA)=8:1 solvent for 30 s and rinsing in IPA for 30 s. After O_2 plasma descum, a chromium adhesion layer (3 nm) and a Au layer (30 nm) were subsequently deposited in vacuum over the pattern. Finally, a well patterned Au nanodisk array on the ITO glass substrate was produced by removing the resist in N,N-dimethylacetamide solution.

A monolayer of hexadecyl trimethyl ammonium bromide was self-assembled on both the bare ITO glass and the substrate with nanodisk array. These two substrates, serving as electrodes, were assembled together to form a LC cell. The cell thickness was controlled to be ~2 μm using the polystyrene microbeads. After injection of LCs, the homeotropic alignment of LCs was achieved. The DFLC material used was MLC-2048 (Merck), which has the positive sign of dielectric anisotropy, $\Delta\varepsilon=\varepsilon_{\parallel}-\varepsilon_{\perp}>0$, for frequencies f of the applied electric field smaller than the crossover frequency $f_c=12$ kHz (at 20 °C) and has a negative sign, $\Delta\varepsilon<0$, when $f>f_c$.[29] Here $\varepsilon_{\parallel}$ and $\varepsilon_{\perp}$ are the dielectric permittivities of the DFLCs in the directions parallel and perpendicular to the LC director, respectively. For LCs with $\Delta\varepsilon>0$, the director prefers to align toward the electric field direction; while for $\Delta\varepsilon<0$, it realigns perpendicularly to the field. DFLCs used in this experiment have an ordinary refractive index $n_o=1.4978$, and an optical birefringence of the material $\Delta n=0.2214$ at $\lambda=589$ nm, namely, $n_e=1.7192$.

A field emission scanning electron microscope (FE-SEM) image of the fabricated nanodisk array is shown in Fig. 1, from which it is determined that the array has an average period of ~290 nm and a disk diameter of ~100 nm. The whole working area of the Au nanodisk array is 3.5×3.5 mm^2. Atomic force microscopy (AFM) reveals the height of each disk as ~33 nm, as shown in the inset of Fig. 1.

Extinction spectra under normal incidence of the probe light were recorded before and after embedding nanodisks into the DFLCs (Fig. 2) with an unpolarized white-light

a)Author to whom correspondence should be addressed. Electronic mail: junhuang@psu.edu.

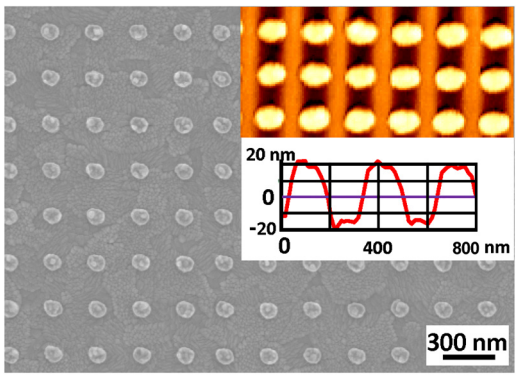

FIG. 1. (Color online) SEM image of an Au nanodisk array on an ITO glass substrate. Inset shows AFM morphologies and height profiles.

beam (HR4000CG-UV-NIR, Ocean Optics). The solid curve is the extinction spectrum of the Au nanodisk array in air, and the dashed curve is the extinction spectrum when the array was embedded in the DFLCs. Upon embedding of the DFLCs, the extinction peak redshifted from 650 to 726 nm and the intensity of the peak increased.

Figures 3(a) and 3(b) show the voltage-dependent extinction spectra when the frequency was fixed at 1 kHz and 18 kHz, respectively. When a low-frequency ($f=1$ kHz) electric field is applied to the cell, the LC molecules with $\Delta\varepsilon>0$ are aligned more orderly (perpendicular to the substrates). In this case, regardless of the polarization of the probe light, it will only see the ordinary refractive index, n_o, of the DFLCs. There is therefore very little changes in the extinction (reduced transmission) caused mainly by more ordered alignment of the positive anisotropic molecules by the applied field [Fig. 3(a)]. When a high-frequency ($f=18$ kHz) voltage is applied, the DFLC exhibits a negative dielectric anisotropy ($\Delta\varepsilon<0$). As the applied voltage exceeds a threshold ($V=10$ V), the LC molecules are switched into horizontal alignment, as illustrated in Fig. 3(b). Here the threshold refers to the voltage that induces the reorientation of the LC molecular layer that is near (generally <100 nm) to the Au nanodisk array.[10] Since LCs do not align perfectly in one direction on the substrate, the probe light will see a combination of n_o and n_e of the DFLCs. For the unpolarized probe light used in our experiment, the effective refractive index at a high frequency can be written as $n_{hf}\cong\sqrt{(n_o^2+n_e^2)/2}=1.6123$, which is larger than that of the homeotropic alignment. Consequently, the extinction peak is redshifted.

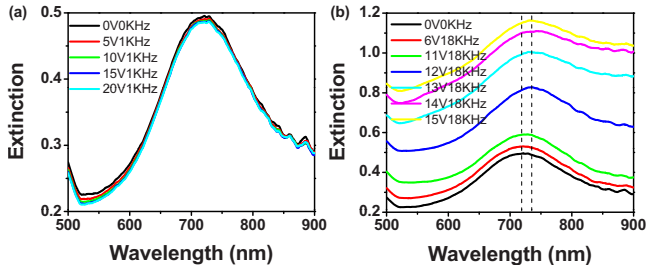

FIG. 3. (Color online) Voltage-dependent extinction spectra with the frequency fixed at (a) 1 kHz and (b) 18 kHz, respectively.

Figure 4 shows the variation in the extinction peak as a function of frequency at a fixed voltage of 12 V. The observed crossover frequency is close to 14 kHz. When the frequency is less than 14 kHz, we can see that there is a ~4 nm blueshift for the extinction peak. At the initial state, the LC molecules are not perfectly aligned, and the refractive index experienced by the probe light will be slightly larger than n_o. When an electric field with low frequency was applied, the LC molecules were aligned more orderly. As a result, the refractive index seen by the probe light will decrease slightly, thereby inducing a small blueshift in the extinction peak. When the frequency of the applied voltage is larger than 14 kHz, the LC molecules start to reorient parallel to the substrates. The probe light will then see an increased refractive index, and the extinction peak redshifts accordingly. From Fig. 4, we observe that there is a ~23 nm redshift when the frequency increases from 15 to 21 kHz. Previous studies have shown that the localized surface plasmon resonance (LSPR) peak shifts linearly as a function of the surrounding refractive index.[30,31] For our specific sample, by comparing LSPR before and after injection of the LCs, we estimate that the sensitivity factor is about 153 nm per refractive index unit. For DFLCs used in this experiment, $n_{hf}=1.6123$, a ~0.11 index increase compared with the perfect homeotropic state is supposed to induce about 17 nm redshift. The larger observed shift, 23 nm, may be caused by the scattering of DFLCs' imperfect alignment near the Au nanodisk arrays. Above 21 kHz, the DFLCs in the cell start to exhibit a multidomain state, which scatters the probe light strongly, thus modifying the extinction spectra. As a result, we observe that the extinction peak drops dramatically and

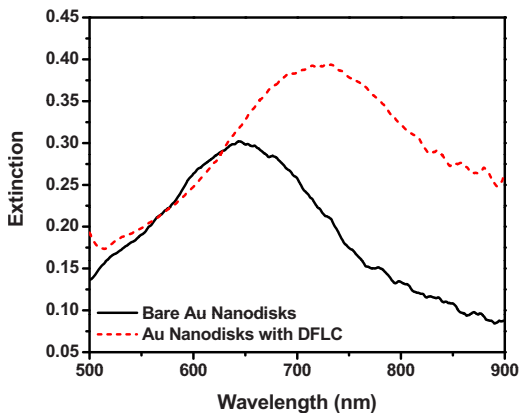

FIG. 2. (Color online) Extinction spectra of a bare Au nanodisk array and an Au nanodisk array embedded in DFLCs.

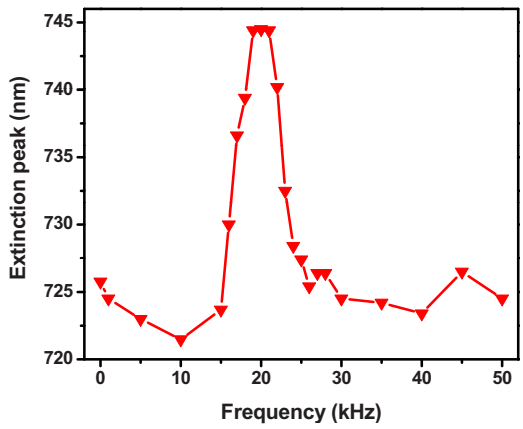

FIG. 4. (Color online) Frequency-dependent extinction peak shift at $V=12$ V.

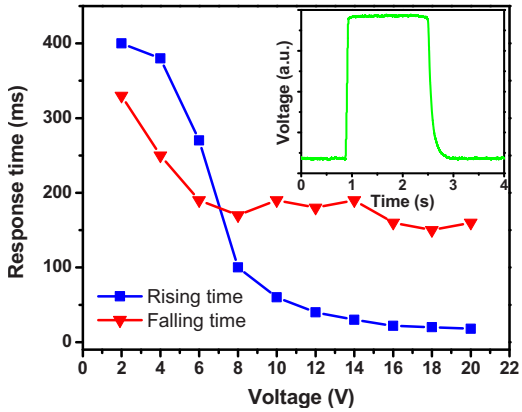

FIG. 5. (Color online) Measured response times under different voltages at fixed frequency of 18 kHz. Inset shows the captured responses of the change in transmitted light intensity.

ultimately approaches a constant value. It is worth mentioning that the LSPR peak shift observed in this plasmonic switch was highly reversible and reproducible with the applied electric field.

Finally we measured the response time of this DFLC-based plasmonic switch. Figure 5 shows the response time under different voltages at a frequency of 18 kHz. The rising time decreases quickly with an increasing voltage and saturates when the voltage is above 12 V. Since the falling time is a self-relaxation process, it is more dependent on the material properties. Above 6 V, the falling time remains almost constant. The optimum rising time and falling time are ~40 ms and 180 ms at 12 V, respectively. The inset shows the responses of the light (633 nm) intensity change captured by an oscilloscope. By employing dual-frequency ac fields, i.e., applying ac fields of two different frequencies to alternatively switch the orientation of the LC between homogeneous state and homeotropic state, the response time that matters is the voltage-dependent "rise" time (~40 ms), which is sufficiently fast for display-related applications. Faster response (response time: <1 ms) can be obtained by using less viscous LCs of higher dielectric anisotropy,[32] or by optical modulation of the nematic birefringence, where the on-times can be much shorter, ranging from the submilliseconds to nanoseconds.[33]

In conclusion, we have demonstrated a frequency-addressed plasmonic switch based on a uniform Au nanodisk array embedded in DFLCs. The frequency-dependent dielectric properties of the DFLCs are the underlying mechanism for the shift in the extinction peak. Exploiting this mechanism, we could engineer the extinction peak of Au nanodisk arrays to blueshift, redshift, or both, by designing the alignment of the DFLC. This DFLC-based active plasmonic system demonstrates an excellent, reversible, and reproducible switching behavior, and it can be potentially used in many applications such as wavelength shifter, polarizers, and color filters.

We gratefully acknowledge the financial support from Air Force Office of Scientific Research (AFOSR), National Science Foundation (NSF), Army Research Office (ARO), and the Penn State Center for Nanoscale Science (MRSEC). Components of this work were conducted at the Penn State node of the NSF-funded National Nanotechnology Infrastructure Network (NNIN). Y.J.L. and Q.H. contribute to this work equally.

[1] R. F. Oulton, V. J. Sorger, T. Zentgraf, R.-M. Ma, C. Gladden, L. Dai, G. Bartal, and X. Zhang, Nature (London) **461**, 629 (2009).
[2] N. Yu, J. Fan, Q. J. Wang, C. Pflugl, L. Diehl, T. Edamura, M. Yamanishi, H. Kan, and F. Capasso, Nat. Photonics **2**, 564 (2008).
[3] S. A. Maier, P. G. Kik, H. A. Atwater, S. Meltzer, E. Harel, B. E. Koel, and A. A. G. Requicha, Nature Mater. **2**, 229 (2003).
[4] A. L. Pyayt, B. Wiley, Y. Xia, A. Chen, and L. Dalton, Nat. Nanotechnol. **3**, 660 (2008).
[5] H. Hu, C. Ma, and Z. Liu, Appl. Phys. Lett. **96**, 113107 (2010).
[6] K. Okamoto, I. Niki, A. Shvartser, Y. Narukawa, T. Mukai, and A. Scherer, Nature Mater. **3**, 601 (2004).
[7] D. M. Koller, A. Hohenau, H. Ditlbacher, N. Galler, F. Reil, F. R. Aussenegg, A. Leitner, E. J. W. List, and J. R. Krenn, Nat. Photonics **2**, 684 (2008).
[8] S. A. Maier and H. A. Atwater, J. Appl. Phys. **98**, 011101 (2005).
[9] B. K. Juluri, Y. B. Zheng, D. Amed, L. Jensen, and T. J. Huang, J. Phys. Chem. C **112**, 7309 (2008).
[10] A. J. Haes, C. L. Haynes, A. D. McFarland, S. Zou, G. C. Schatz, and R. P. Van Duyne, MRS Bull. **30**, 368 (2005).
[11] C. L. Haynes, A. D. McFarland, L. Zhao, R. P. Van Duyne, G. C. Schatz, L. Gunnarsson, J. Prikulis, B. Kasemo, and M. Käll, J. Phys. Chem. B **107**, 7337 (2003).
[12] H. Wang, G. Goodrich, F. Tam, C. Oubre, P. J. Nordlander, and N. J. Halas, J. Phys. Chem. B **109**, 11083 (2005).
[13] Y. B. Zheng, L. Jensen, W. Yan, T. R. Walker, B. K. Juluri, L. Jensen, and T. J. Huang, J. Phys. Chem. C **113**, 7019 (2009).
[14] Y. B. Zheng, T. J. Huang, A. Y. Desai, S. J. Wang, L. K. Tan, H. Gao, and A. C. H. Huan, Appl. Phys. Lett. **90**, 183117 (2007).
[15] P. A. Kossyrev, A. J. Yin, S. G. Cloutier, D. A. Cardimona, D. H. Huang, P. M. Alsing, and J. M. Xu, Nano Lett. **5**, 1978 (2005).
[16] J. Dintinger, I. Robel, P. V. Kamat, C. Genet, and T. W. Ebbesen, Adv. Mater. (Weinheim, Ger.) **18**, 1645 (2006).
[17] W. Dickson, G. A. Wurtz, P. R. Evans, R. J. Pollard, and A. V. Zayats, Nano Lett. **8**, 281 (2008).
[18] V. K. S. Hsiao, Y. B. Zheng, B. K. Juluri, and T. J. Huang, Adv. Mater. (Weinheim, Ger.) **20**, 3528 (2008).
[19] Y. B. Zheng, Y.-W. Yang, L. Jensen, L. Fang, B. K. Juluri, A. H. Flood, P. S. Weiss, J. F. Stoddart, and T. J. Huang, Nano Lett. **9**, 819 (2009).
[20] B. K. Juluri, M. Q. Lu, Y. B. Zheng, T. J. Huang, and L. Jensen, J. Phys. Chem. C **113**, 18499 (2009).
[21] Y. J. Liu, Y. B. Zheng, J. J. Shi, H. Huang, T. R. Walker, and T. J. Huang, Opt. Lett. **34**, 2351 (2009).
[22] A. V. Krasavin and N. I. Zheludev, Appl. Phys. Lett. **84**, 1416 (2004).
[23] K. F. MacDonald, Z. L. Samson, M. I. Stockman, and N. I. Zheludev, Nat. Photonics **3**, 55 (2009).
[24] V. V. Temnov, G. Armelles, U. Woggon, D. Guzatov, A. Cebollada, A. Garcia-Martin, J.-M. Garcia-Martin, T. Thomay, A. Leitenstorfer, and R. Bratschitsch, Nat. Photonics **4**, 107 (2010).
[25] Y.-H. Fan, H. Ren, X. Liang, Y.-H. Lin, and S.-T. Wu, Appl. Phys. Lett. **85**, 2451 (2004).
[26] C.-H. Wen and S.-T. Wu, Appl. Phys. Lett. **86**, 231104 (2005).
[27] E. Graugnard, S. N. Dunham, J. S. King, D. Lorang, S. Jain, and C. J. Summers, Appl. Phys. Lett. **91**, 111101 (2007).
[28] E. Graugnard, J. S. King, and C. J. Summers, Y. Zhang-Williams, and I. C. Khoo, Phys. Rev. B **72**, 233105 (2005).
[29] O. Pishnyak, S. Sato, and O. D. Lavrentovich, Appl. Opt. **45**, 4576 (2006).
[30] A. D. McFarland and R. P. Van Duyne, Nano Lett. **3**, 1057 (2003).
[31] Y. B. Zheng, B. K. Juluri, X. Mao, T. R. Walker, and T. J. Huang, J. Appl. Phys. **103**, 014308 (2008).
[32] A. B. Golovin, S. V. Shiyanovskii, and O. D. Lavrentovich, Appl. Phys. Lett. **83**, 3864 (2003).
[33] I. C. Khoo, Phys. Rep. **471**, 221 (2009).